Contents

1 The Proposed Experiment **2**
1.1 A_{zz} Experimental Method 2
1.2 Kinematics 3

1 The Proposed Experiment

We propose to measure the tensor asymmetry A_{zz} and tensor analyzing power T_{20} from inclusive electron scattering from polarized deuterons in the quasi-elastic and elastic region of $0.80 < x < 1.75$, 1.0 (GeV/c)$^2 < Q^2 < 1.9$ (GeV/c)^2, and $0.59 < W < 1.09$ GeV using the Hall C HMS and SHMS spectrometers at forward angle using a solid polarized ND_3 target.

1.1 A_{zz} Experimental Method

The measured double differential cross section for a spin-1 target is characterized by a vector polarization P_z and tensor polarization P_{zz} is expressed as,

$$\frac{d^2\sigma_p}{d\Omega dE'} = \frac{d^2\sigma_u}{d\Omega dE'}\left(1 - P_z P_B A_1 + \frac{1}{2}P_{zz}A_{zz}\right), \tag{1}$$

where, σ_p (σ_u) is the polarized (unpolarized) cross section, P_B is the incident electron beam polarization, and A_1 (A_{zz}) is the vector (tensor) asymmetry of the virtual-photon deuteron cross section. This allows us to write the polarized tensor asymmetry with positive tensor polarization using an unpolarized electron beam as

$$A_{zz} = \frac{2}{P_{zz}}\left(\frac{\sigma_p - \sigma_u}{\sigma_u}\right). \tag{2}$$

The tensor polarization is given by

$$P_{zz} = \frac{n_+ - 2n_0 + n_-}{n_+ + n_- + n_0}, \tag{3}$$

where n_m represents the population in the $m_z = +1$, -1, or 0 state.

Eq. 2 reveals that the asymmetry A_{zz} compares two different cross sections measured under different polarization conditions of the target: positively tensor polarized and unpolarized. To obtain the relative cross section measurement in the same configuration, the same target cup and material will be used at alternating polarization states (polarized vs. unpolarized), and the magnetic field providing the quantization axis will be oriented along the beamline at all times. This field will always be held at the same value, regardless of the target material polarization state. This process, identical to that used for the E12-13-011 b_1 measurement, ensures that the acceptance remains consistent within the stability (10^{-4}) of the super conducting magnet.

Since many of the factors involved in the cross sections cancel in the ratio, Eq. 2 can be expressed in terms of the charge normalized, efficiency corrected numbers of tensor polarized (N_p) and unpolarized (N_u) counts,

$$A_{zz} \;=\; \frac{2}{fP_{zz}}\left(\frac{N_p - N_u}{N_u}\right). \tag{4}$$

The dilution factor f corrects for the presence of unpolarized nuclei in the target and is defined by

$$f = \frac{N_D\sigma_D}{N_N\sigma_N + N_D\sigma_D + \sum\limits_A N_A\sigma_A}, \tag{5}$$

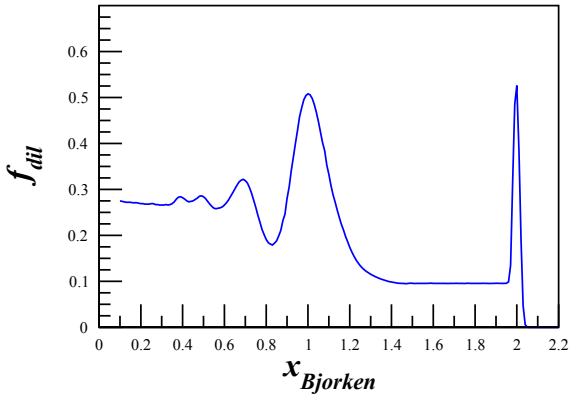

Figure 1: The estimated dilution factor, in this case at $Q^2 = 1.5\ (\mathrm{GeV}/c)^2$, is expected to drop off at high x until it reaches the SRC plateau region and then the elastic peak at $x = 2$. The low dilution factor of $1.1 < x < 1.95$ will be counteracted by using a high-luminosity target.

where N_D is the number of deuterium nuclei in the target and σ_D is the corresponding inclusive double differential scattering cross section, N_N is the nitrogen number of scattered nuclei with cross section σ_N, and N_A is the number of other scattering nuclei of mass number A with cross section σ_A. As has been noted in previous work [1], the dilution factor at high x drops off considerably until the SRC plateau region, as shown in Fig. 1. By using a high-luminosity solid target and a low scattering angle $\theta_{e'}$, this effect will be counteracted. The dilution factor is a much smaller problem for elastic scattering at $x = 2$.

The dilution factor can be written in terms of the relative volume ratio of ND_3 to LHe in the target cell, otherwise known as the packing fraction p_f. In our case of a cylindrical target cell oriented along the magnetic field,the packing fraction is exactly equivalent to the percentage of the cell length filled with ND_3.

If the time is evenly split between scattering off of polarized and unpolarized ND_3, the time necessary to achieve the desired precision δA is:

$$T = \frac{N_p}{R_p} + \frac{N_u}{R_u} = \frac{8}{f^2 P_{zz}^2} \left(\frac{R_p(R_u + R_p)}{R_u^3} \right) \frac{1}{\delta A_{zz}^2} \tag{6}$$

where $R_{p(u)}$ is the polarized (unpolarized) rate and $N_{p(u)}$ is the total estimated number of polarized (unpolarized) counts to achieve the uncertainty δA_{zz}.

1.2 Kinematics

We propose to measure the tensor asymmetry A_{zz} for $0.80 < x < 1.75$, $1.0\ (\mathrm{GeV}/c)^2 < Q^2 < 1.9\ (\mathrm{GeV}/c)^2$, and $0.59 < W < 1.09$ GeV after applying kinematics cuts. Fig. 2 shows the planned kinematic coverage utilizing the Hall C HMS and SHMS spectrometers at forward angle.

The polarized ND_3 target is discussed in section **??**. The magnetic field of the target will be held constant along the beamline at all times, while the target state is alternated between a polarized

		E_0 (GeV)	Q^2 (GeV^2)	E' (GeV)	$\theta_{e'}$ ($^\circ$)	Rates (kHz)	PAC Time (Days)
SHMS	(S1)	8.8	1.5	8.36	8.2	0.38	25
HMS	(H1)	8.8	2.9	7.26	12.2	0.04	25
SHMS	(S2)	6.6	0.7	6.35	7.5	3.57	8
HMS	(H2)	6.6	1.8	5.96	12.3	0.09	8
SHMS	(S3)	2.2	0.2	2.15	10.9	10.5	1
HMS	(H3)	2.2	0.3	2.11	14.9	3.23	1

Table 1: Summary of the central kinematics and physics rates using the Hall C spectrometers.

	H1: $Q^2 = 2.9$ (GeV/c)^2			H2: $Q^2 = 1.8$ (GeV/c)^2			S1: $Q^2 = 1.5$ (GeV/c)^2		
x	f_{dil}	δA_{zz}^{stat} $\times 10^{-2}$	δA_{zz}^{sys} $\times 10^{-2}$	f_{dil}	δA_{zz}^{stat} $\times 10^{-2}$	δA_{zz}^{sys} $\times 10^{-2}$	f_{dil}	δA_{zz}^{stat} $\times 10^{-2}$	δA_{zz}^{sys} $\times 10^{-2}$
0.50	0.29	2.02	1.84	—	—	—	0.25	0.72	1.84
0.60	0.29	0.91	????	0.27	3.22	????	0.30	0.36	????
0.70	0.27	1.01	????	0.32	1.26	????	0.29	0.38	????
0.80	0.30	1.11	1.34	0.20	2.02	0.48	0.17	0.74	1.34
0.90	0.24	1.73	0.38	0.27	1.45	1.10	0.29	0.44	0.38
1.00	0.46	1.03	????	0.50	0.74	????	0.51	0.24	????
1.10	0.28	2.48	0.14	0.32	1.68	1.67	0.34	0.49	0.14
1.20	0.09	11.7	1.55	0.16	5.14	3.41	0.17	1.34	1.55
1.30	0.11	16.8	4.13	0.12	10.6	5.12	0.12	2.79	4.13
1.40	—	—	—	0.11	18.4	6.86	0.13	4.30	6.72
1.50	—	—	—	—	—	—	0.10	7.01	8.34
1.60	—	—	—	—	—	—	0.10	9.60	8.42
1.70	—	—	—	—	—	—	0.10	12.7	7.04
1.80	—	—	—	—	—	—	0.10	16.6	4.72
2.00	—	—	—	—	—	—	0.50	2.79	9.20

Table 2: Summary of the expected uncertainty for each x bin for settings S1, H1, and H2.

	S2: $Q^2 = 0.7$ $(\mathrm{GeV}/c)^2$			H3: $Q^2 = 0.3$ $(\mathrm{GeV}/c)^2$			S3: $Q^2 = 0.2$ $(\mathrm{GeV}/c)^2$		
x	f_{dil}	δA_{zz}^{stat} $\times 10^{-2}$	δA_{zz}^{sys} $\times 10^{-2}$	f_{dil}	δA_{zz}^{stat} $\times 10^{-2}$	δA_{zz}^{sys} $\times 10^{-2}$	f_{dil}	δA_{zz}^{stat} $\times 10^{-2}$	δA_{zz}^{sys} $\times 10^{-2}$
0.30	0.24	0.99	1.84	—	—	—	0.18	2.13	1.84
0.40	0.28	0.26	1.84	—	—	—	0.12	1.38	1.84
0.50	0.32	0.21	1.84	0.14	3.52	1.84	0.11	1.23	1.84
0.60	0.19	0.41	????	0.12	2.26	????	0.18	0.78	????
0.70	0.13	0.68	????	0.18	1.33	????	0.28	0.48	????
0.80	0.19	0.48	0.48	0.30	0.72	0.48	0.42	0.31	0.48
0.90	0.39	0.22	1.10	0.46	0.45	1.10	0.54	0.24	1.10
1.00	0.52	0.16	????	0.52	0.43	????	0.58	0.25	????
1.10	0.39	0.28	1.27	0.43	0.63	1.07	0.53	0.33	0.95
1.20	0.22	0.65	2.54	0.30	1.15	2.14	0.40	0.55	1.91
1.30	0.14	1.34	3.81	0.19	2.16	3.22	0.32	0.83	2.87
1.40	0.09	2.29	5.06	0.14	3.52	4.29	0.24	1.31	3.82
1.50	0.06	4.09	6.35	0.10	5.85	5.37	0.20	1.86	4.78
1.60	0.04	7.76	7.60	0.06	10.4	6.45	0.14	2.87	5.74
1.70	0.04	9.23	8.88	0.05	13.5	7.52	0.10	4.53	6.69
1.80	0.03	14.9	9.20	0.06	13.9	8.60	0.11	4.73	7.66
2.00	0.67	3.79	9.20	0.20	3.05	9.20	0.70	0.45	9.20

Table 3: Summary of the expected uncertainty for each x bin for settings S2, S3, and H3.

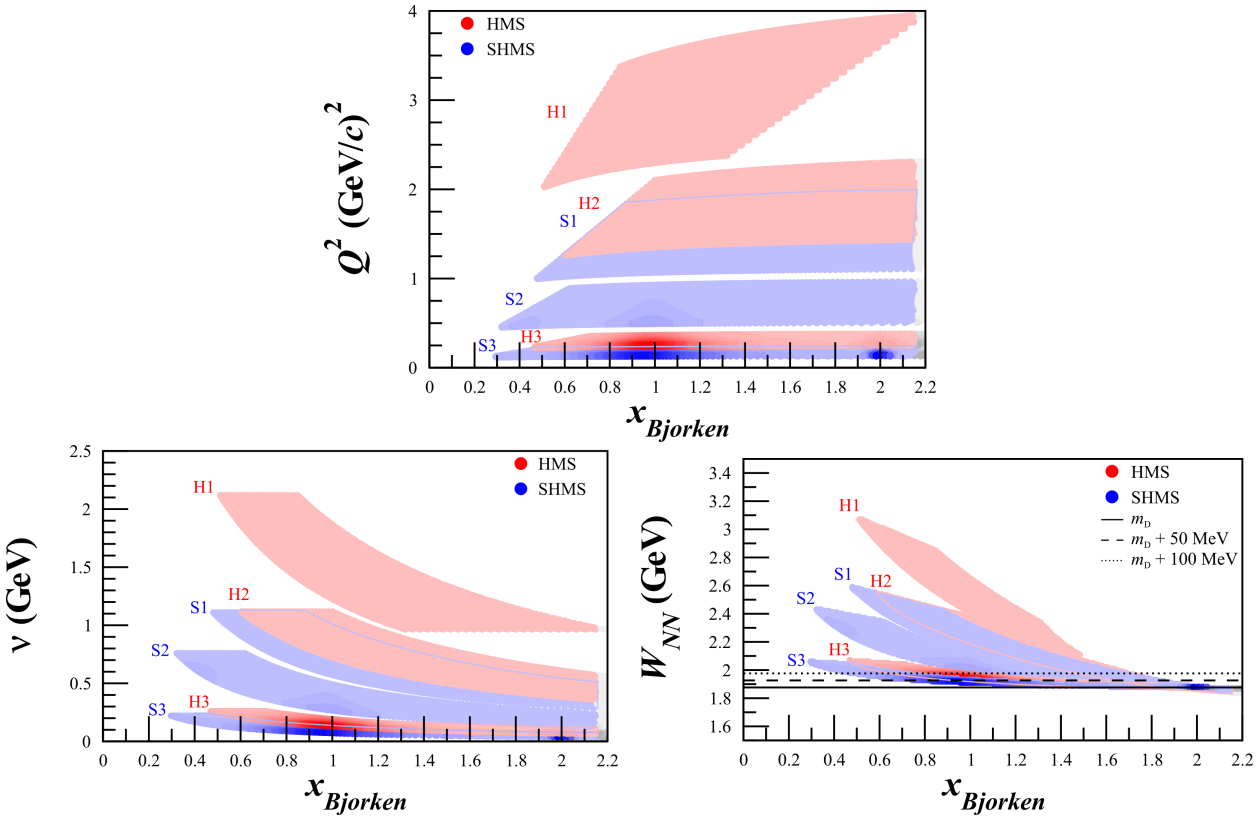

Figure 2: Kinematic coverage for central spectrometer settings at $Q^2 = 1.5$ $(\mathrm{GeV}/c)^2$ (A), 0.7 $(\mathrm{GeV}/c)^2$ (B), and 0.3 $(\mathrm{GeV}/c)^2$ (C). The HMS is only used for setting C, and its coverage largely falls under the SHMS coverage. The grey regions are not included in our statistics estimates since they fall outside of $0.80 < x < 1.75$. Darker shading represents areas with higher statistics, and the dotted line in the W plot indicates nucleon mass.

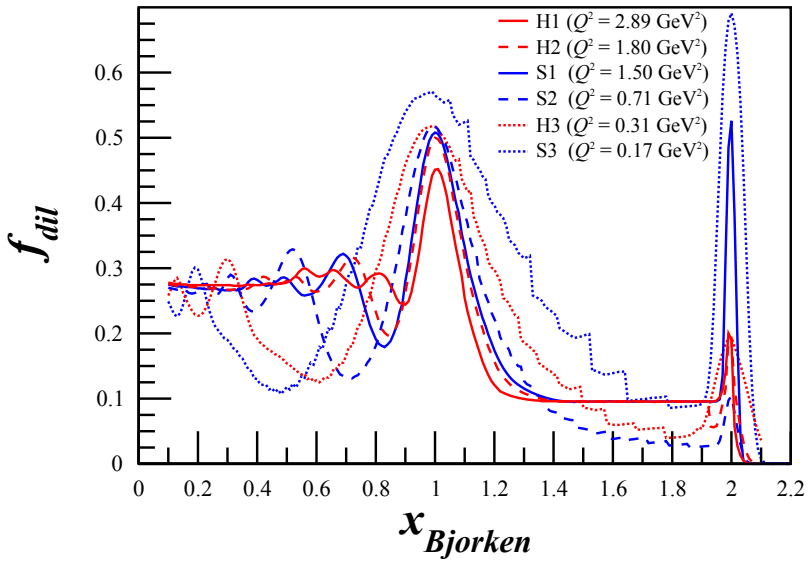

Figure 3: Projected dilution factor covering the entire x range to be measured using a combination of P. Bosted's [2] and M. Sargsian's [3] code, along with a calculation of the elastic peak using a parametrization of the deuteron form factors, for the SHMS and HMS.

and unpolarized state. The tensor polarization and packing fraction used in the rates estimate are 30% and 0.65, respectively. The dilution fraction in the range of this measurement is shown in Fig. 3. With an incident electron beam current of 90 nA, the expected deuteron luminosity is 1.3×10^{35} cm^{-2}s^{-1}.

The momentum bite and the acceptance were assumed to be $\Delta P = \pm 8\%$ and $\Delta\Omega = 5.6$ msr for the HMS, and $\Delta P = ^{+20\%}_{-8\%}$ and $\Delta\Omega = 4.4$ msr for the SHMS. For the choice of the kinematics, special attention was taken onto the angular and momentum limits of the spectrometers with a longitudinal polarized target: for the HMS, $12.2^\circ \leq \theta \leq 85^\circ$ and $1 \leq P_0 \leq 7.3$ GeV/c, and for the SHMS, $5.5^\circ \leq \theta \leq 40^\circ$ and $2 \leq P_0 \leq 11$ GeV/c. In addition, the opening angle between the spectrometers is physically constrained to be larger than 17.5°. The dilution factors and projected uncertainties in A_{zz} are summarized in Tables 2-3 and displayed in Fig. 4.

A total of 30 days of beam time is requested for production data, with an additional 9.1 days of expected overhead.

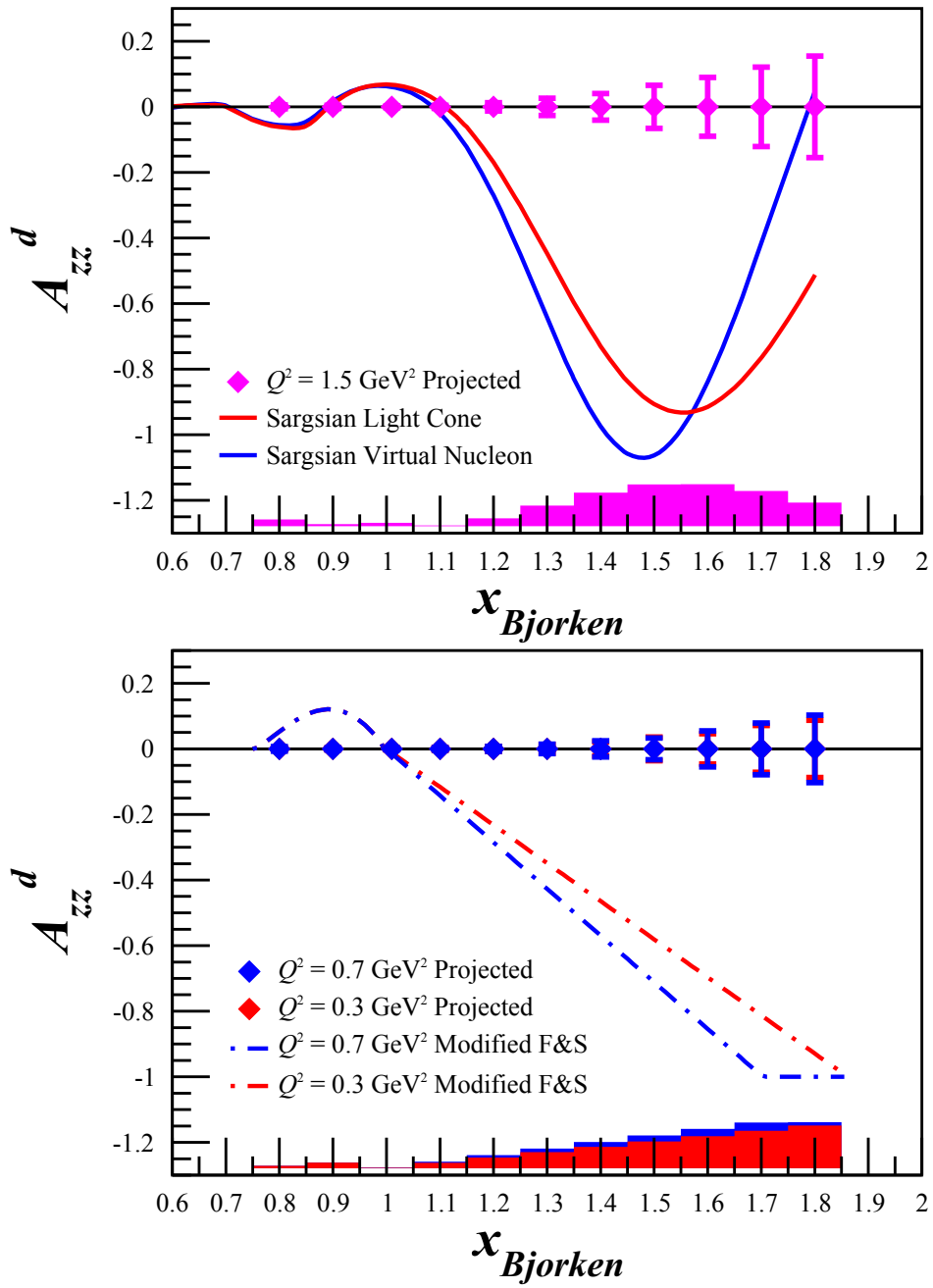

Figure 4: Projected statistical errors for the tensor asymmetry A_{zz} with 30 days of beam time. The band represents the systematic uncertainty. Also shown for $Q^2 = 1.5$ $(\mathrm{GeV}/c)^2$ are calculations provided by M. Sargsian for using a light cone and virtual nucleon model, and for $Q^2 = 0.3$ and 0.7 $(\mathrm{GeV}/c)^2$ a modified Frankfurt and Strikman model [1] that estimates the peak shifts in x expected due to the SRC scaling changing with Q^2 [4].

References

[1] L. Frankfurt and M. Strikman, Phys.Rept. **160**, 235 (1988).

[2] P. Bosted and V. Mamyan, e-print **arXiv:1203.2262**, (2012).

[3] M. Sargsian, private communication.

[4] L. Frankfurt, M. Sargsian, and M. Strikman, Int.J.Mod.Phys. **A23**, 2991 (2008).